Coupled-Mode Design of Ferrite-Loaded Coupled-Microstrip-Lines Section

Jerzy Mazur, Mateusz Mazur, and Jerzy Michalski

***Abstract*—A coupled-mode approach is applied to a microstrip circulator with a distributed section of axially magnetized ferrite coupled lines (FCLs). The equivalent model of the FCL junction is found, which includes gyromagnetic interaction between propagated and evanescent isotropic modes. On the basis of the coupling process, the ferrite modes in the FCL are defined. From the decomposition of these modes, the waves in each line of the structure are determined. The mode matching is applied at the junction ports, which allows one to obtain the scattering matrix of the microstrip FCL. Validity of the approach is verified by checking the scattering parameters of the FCL section and comparing the numerical results with available measurements. The proposed model gives the properties with regards to the impedance matching and ferrite section dimensions, which can help the design of the FCL nonreciprocal devices. As an example, the S-parameters of an FCL circulator are presented.**

***Index Terms*—Circulators, ferrite-coupled-lines junction, scattering matrix.**

I. Introduction

THE distributed circulators and isolators, which make use of the coupled slot-lines sections with an axially magnetized ferrite, were discovered in [1]. The operation principle of these devices has been explained in [2] and [3] using the bimode coupled-mode (CM) model employing the Faraday's rotation phenomenon appearing in the ferrite coupled lines (FCLs). It was found that although the Faraday's effect assured only the nonreciprocal phase shift, the section of FCL demonstrated full nonreciprocal properties when the structure was fed by even or odd excitations. Thus, these requirements are satisfied in FCL devices [3], which are constructed as a cascade of an FCL section with $0^\circ/180^\circ$ hybrid junction. One should note here that the overall performance of these nonreciprocal devices depends on the appropriate scattering characteristics of the individual components. Using the CM model of FCL lines, the scattering matrix of the FCL section has been derived in [2] and [3]. However, there is no analysis of the matching conditions without which the proper compact of the FCL with external sections cannot be designed. Teoh and Davis have presented in [4] and [5] the different attempts to solve the problem in terms of superposition of the dominant ferrite modes propagating along the FCL. Their normal mode approach confirmed the CM operation conditions of the FCL. However, the matching problem was also neglected. Therefore, the satisfactory design procedure of FCL junctions in principle has not been achieved. Recently, Xie and Davis [6] have examined the reflection and power transfer of the even and odd isotropic modes at the interface between the coupled isotropic and ferrite lines. They solved the problem using the mode-matching approach where the dominant modes of the cascaded dielectric and ferrite lines were applied in the field expansion. However, their solution has omitted the excitation of the interface by the ferrite modes so that the scattering problem at the considered interface has been only partially analyzed. Hence, their theoretical prediction is applicable to the case when the second interface of the FCL section is perfectly matched. We can conclude, therefore, that the scattering problem of the magnetized FCL section has not yet been solved sufficiently.

In this paper, the mode-matching approach is also applied to define, for the first time, the scattering matrix of the FCL section. The problem is solved by matching the fields of isotropic and ferrite modes at both of the interfaces of the section. The ferrite modes are defined using the CM model of the ferrite microstrip lines [9], where these modes are performed by gyromagnetic coupling of the propagating and evanescent isotropic modes. The fields at the ferrite region are defined by two forward and backward traveling dominant and evanescent higher order ferrite modes. The two dominant and two higher order evanescent isotropic modes are taken into account as input and output waves at the isotropic regions of the structure. The decomposition of these modes into the waves, appearing at the microstrip ports of the junction, makes it possible to incorporate their eigenfields into a matching process at each port's interface. In this way, the complete scattering matrix of the FCL structure is finally formulated. The usefulness of the developed theory is demonstrated by the comparison of the scattering characteristics calculated for the FCL microstrip section with experimental ones presented by Davis *et al.* in [7]. The overall scattering characteristics of the microstrip circulator comprising the investigated FCL section in cascade with a microstrip T-junction are also presented.

II. CM Model of FCL

The investigated guide is assumed to be a symmetrical structure of lossless coupled lines with a slab of an axially magnetized ferrite, as shown in Fig. 1. The transverse fields $\vec{E}_t$ and $\vec{H}_t$ in the guide are expressed in terms of eigenfunctions $\vec{e}_t, \vec{h}_t$ of a second base isotropic waveguide. According to the CM procedure [8], the Maxwell's equations of both guides are combined

Manuscript received October 17, 2000. This work was supported in part by the Telecommunications Research Institute under Grant DN-24204.

J. Mazur is with the Technical University of Gdańsk and Telecommunications Research Institute, 81-952 Gdańsk, Poland (e-mail: jem@pg.gda.pl).

M. Mazur and J. Michalski are with the Telecommunications Research Institute, 81-952 Gdańsk, Poland (e-mail: mefis@pit.gda.pl; MichalskiJ@prokom.pl).

Publisher Item Identifier S 0018-9480(02)05203-1.

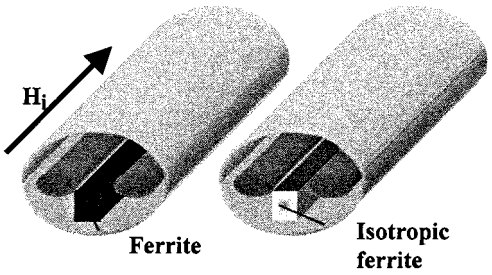

Fig. 1. Coupled lines loaded with a slab of an axially magnetized ferrite. (a) Ferrite guide. (b) Corresponding dielectric basis guide.

together and integrated over the cross section of the investigated structure.

Due to the orthogonality of the base eigenfunctions, the integral equations are reduced to a matrix eigenvalue problem, and solutions correspond to the modal fields and propagation constants of the ferrite guide. The resulting system of linear equations has the ordinary form [9] written as

$$\frac{\partial U_n}{\partial z} + j\beta_n Z_n I_n = -jK_n - \sum_n I_m C_{mn}$$
$$\frac{\partial I_n}{\partial z} + j\beta_n Y_n U_n = 0 \tag{1}$$

where

$$K_n = k_0\eta_0(\mu - \mu_z)\int_{\Omega_f} \vec{h}_{tn}\cdot\vec{h}^*_{tn}d\Omega_f \tag{2}$$

$$C_{mn} = k_0\eta_0\mu_a\int_{\Omega_f} \vec{h}_{tm}\times\vec{h}^*_{tn}d\Omega_f \tag{3}$$

k_0 and η_0 denote the wavenumber and intrinsic impedance in vacuum, and β_n, Z_n, and Y_n are the propagation constant, wave impedance, and the wave admittance of the nth isotropic mode, respectively. μ, μ_z are diagonal elements and μ_a is the off-diagonal element in the relative permeability tensor of the ferrite. The coefficient K_n defines the perturbation of the nth isotropic mode, while the coefficient C_{mn} determines the gyromagnetic coupling between the nth and mth isotropic modes. The coupling occurs in the ferrite region Ω_f where the transverse $\vec{h}_{tm}$ and $\vec{h}_{tn}$ vectors are perpendicular to each other. Moreover, the following condition for the coupling coefficients is satisfied, i.e., $C_{nm} = -C^*_{mn}$. The unknown voltage U_n and current I_n coefficients are functions of z only, with z dependence e^{-jkz}, where k is propagation constant.

III. Scattering Matrix of Microstrip FCL

Following the above outlined model, the coupled ferrite microstrips shown in Fig. 2 are first investigated. It is assumed that the ferrite is weakly magnetized, thus, $\mu = \mu_z = 1$ and coefficient $K_n = 0$ in (1). Additionally, it was found in [9] that at least four isotropic modes sufficiently define the CM model of the microstrip FCL. There are two dominant even $\underline{\mathbf{1}}$ and odd $\underline{\mathbf{2}}$ quasi-TEM modes and two higher modes, which correspond to the even $\underline{\mathbf{3}}$ and odd $\underline{\mathbf{4}}$ quasi-TE_1 waves, and only these modes are used in the field expansion. Applying the distribution of the magnetic-field vectors $\vec{h}_{ti}$ of isotropic modes, shown in Fig. 3,

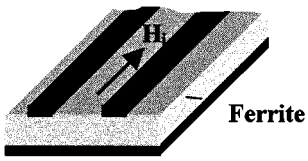

Fig. 2. Structure of microstrip FCLs.

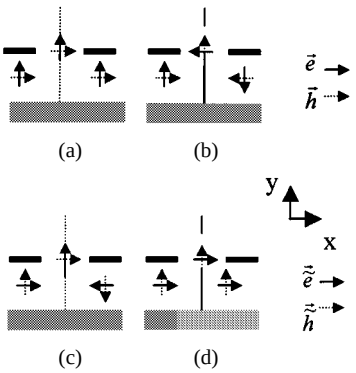

Fig. 3. Schematic distribution of the transverse electric and magnetic fields of isotropic modes in the cross section of the FCL. (a) Even dominant mode $\underline{\mathbf{1}}$. (b) Odd dominant odd $\underline{\mathbf{2}}$. (c) Higher order even mode $\underline{\mathbf{3}}$. (d) Higher order odd mode $\underline{\mathbf{4}}$. Symmetry plane: magnetic wall for even modes and electric wall for odd modes.

to (3), we expect that the coupling of dominant modes as well as of the higher ones can appear only in the ferrite region situated near the slot between the strips. Moreover, the additional coupling of the dominant even (odd) mode and higher odd (even) mode can occur in the ferrite regions beneath the strips. If we include the above assumptions into CM equations and assume the wave propagation along the ferrite guide as e^{-jkz}, then (1) can be reduced to the following matrix forms:

$$\begin{bmatrix} k^2-\beta_1^2 & jC_{12}\beta_2Y_2 & 0 & jC_{14}\beta_4Y_4 \\ -jC_{12}\beta_1Y_1 & k^2-\beta_2^2 & jC_{12}\beta_2Y_2 & 0 \\ 0 & -jC_{23}\beta_2Y_2 & k^2-\beta_3^2 & jC_{34}\beta_4Y_4 \\ -jC_{14}\beta_1Y_1 & 0 & -jC_{34}\beta_3Y_3 & k^2-\beta_4^2 \end{bmatrix} \cdot \begin{bmatrix} U_1 \\ U_2 \\ U_3 \\ U_4 \end{bmatrix} = 0 \tag{4a}$$

and

$$\begin{bmatrix} I_1 \\ I_2 \\ I_3 \\ I_4 \end{bmatrix} = \begin{bmatrix} \frac{\beta_1Y_1}{k} & 0 & 0 & 0 \\ 0 & \frac{\beta_2Y_2}{k} & 0 & 0 \\ 0 & 0 & \frac{\beta_3Y_3}{k} & 0 \\ 0 & 0 & 0 & \frac{\beta_4Y_4}{k} \end{bmatrix} \cdot \begin{bmatrix} U_1 \\ U_2 \\ U_3 \\ U_4 \end{bmatrix} \tag{4b}$$

where $\beta_{1(2)}$ and $\beta_{3(4)}$ are known propagation constants of the dominant and higher isotropic modes, respectively. Their wave admittance is defined as follows, i.e., $Y_{1(2)} = \beta_{1(2)}/k_0\eta_0$ and $Y_{3(4)} = \beta_{3(4)}/k_0\eta_0$. The quantities $C_{ij}, i, j = 1, \ldots, 4$ are coupling coefficients of isotropic modes. The propagation constant k of the CMs is found by equating the determinant of the coefficient matrix of (4a) to zero. It yields the four eigenvalues of (4a) defining propagation constants $k_{1(2)}$ of fundamental and $k_{3(4)}$ of higher order ferrite modes for both $(\pm z)$ propagation directions. On the other hand, if the propagation

constants k_i are known, then the characteristic equation of (4a) can be turned on to yield the coupling coefficients. The requirement that the determinant of (4a) is zero for each value of $k_i, i = 1,\ldots,4$ yields the set of four nonlinear algebraic equations for $C_{ij}, i,j = 1,\ldots,4$, which can be solved numerically. To verify the solutions, we need the approximate values of the coupling coefficients. It can be found using (2) or the effective mode formulation proposed in [9]. The eigenfunctions of (4a) corresponding to the eigenvalues $\pm k_i, i = 1,\ldots,4$ define the complete z dependence of the modal voltages $\underline{U}(z) = [U_1(z), U_2(z), U_3(z), U_4(z)]^T$ of the ferrite modes given by

$$\underline{U}(z) = \underline{\underline{M}}\Big(\mathrm{diag}(e^{-jk_iz})\underline{A}_F + \mathrm{diag}(e^{ik_iz})\underline{A}_B\Big) \quad (5)$$

where

$$\underline{\underline{M}} = \begin{bmatrix} 1 & M_{12} & M_{13} & M_{14} \\ M_{21} & 1 & M_{23} & M_{24} \\ M_{31} & M_{32} & 1 & M_{34} \\ M_{41} & M_{42} & M_{43} & 1 \end{bmatrix}$$

and

$$\mathrm{diag}(e^{\mp k_iz}) = \begin{bmatrix} e^{\mp jk_1z} & 0 & 0 & 0 \\ 0 & e^{\mp jk_2z} & 0 & 0 \\ 0 & 0 & e^{\mp jk_3z} & 0 \\ 0 & 0 & 0 & e^{\mp jk_4z} \end{bmatrix}.$$

In addition, $\underline{A}_{F(B)} = [A_1, A_2, A_3, A_4]^T_{F(B)}$ are unknown constants. Suppose we apply the eigenfunction of ith mode as a partial voltage source $V_i = Ae^{-jk_iz}$. The response $U_{ji}, j = 1,\ldots,4$ will then be the jth partial field voltage of the ith mode due to source V_i. Hence, the coefficients $M_{ii} = 1$ and $M_{ji} = U_{ji}/V_i$ are the nondimensional terms.

Applying (5) in (4b), the vector of modal currents $\underline{I}(z) = [I_1(z), I_2(z), I_3(z), I_4(z)]^T$ is defined as

$$\underline{I}(z) = \underline{\underline{Y}}\Big(\mathrm{diag}(e^{-jk_iz})\underline{A}_F - \mathrm{diag}(e^{-jk_iz})\underline{A}_B\Big), \quad i = 1,\ldots,4. \quad (6)$$

In matrix $\underline{\underline{Y}}$, the elements $Y_{ji} = (\beta_jY_j)/(k_i)M_{ji}, j,i = 1,\ldots,4$ are the partial transfer wave admittance for $j \neq i$ and the ith mode wave admittance for $j = i$. According to the mode expansion, the electric and magnetic fields in the ferrite section taken as the superposition of the four normal ferrite modes can be expressed as

$$\vec{E}_t = \sum_{i=1}^{4} U_i(z)\vec{e}_{ti}$$
$$\vec{H}_t = \sum_{i=1}^{4} I_i(z)\vec{h}_{ti} \quad (7)$$

where $\vec{e}_{ti}$ and $\vec{h}_{ti}$ are eigenvectors of the transverse electric and magnetic fields of isotropic modes.

To decompose the fields $\vec{E}_t$ and $\vec{H}_t$ into two lines constituting the FCL section, we consider the schematic distribution of $\vec{h}_{ti}$ and $\vec{e}_{ti}$ depicted in Fig. 3. It is seen that the eigenfields of dominant even $\underline{\mathbf{1}}$ and odd $\underline{\mathbf{2}}$ modes have e_y and h_x components associated with each of the lines. Similar components of the higher even $\underline{\mathbf{3}}$ and odd $\underline{\mathbf{4}}$ modes are e_x and h_y. The symmetry plane of the isotropic guide is defined as the magnetic and electric wall for the even and odd modes, respectively. Therefore, we can assume that the values of these components for the dominant modes, as well as for the higher order ones, are equal at the both lines. Moreover, the eigenfields of the dominant even and the higher odd modes are in-phase, while they are 180° out-of-phase for the dominant odd mode and higher even one. Making use of the above fields properties in (7), the distribution of the electric $\vec{E}$ and magnetic $\vec{H}$ fields along both lines can be written as

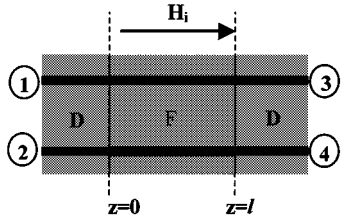

Fig. 4. Top view of the microstrip FCL junction consisting of input dielectric (D) and ferrite (F) sections. This configuration was proposed by Davis *et al.* in [7].

$$\vec{E}_t^1(z) = \big(U_1(z) + U_2(z)\big)\vec{e} + \big(U_3(z) + U_4(z)\big)\vec{\tilde{e}}$$
$$\vec{E}_t^2(z) = \big(U_1(z) - U_2(z)\big)\vec{e} + \big(U_3(z) - U_4(z)\big)\vec{\tilde{e}}$$
$$\vec{H}_t^1(z) = \big(I_1(z) + I_2(z)\big)\vec{h} + \big(I_3(z) + I_4(z)\big)\vec{\tilde{h}}$$
$$\vec{H}_t^2(z) = \big(I_1(z) - I_2(z)\big)\vec{h} + \big(I_3(z) - I_4(z)\big)\vec{\tilde{h}} \quad (8)$$

where superscripts 1 and 2 denote the FCL lines, and $(e,h) \sim (e_y,h_x)$ and $(\tilde{e},\tilde{h}) \sim (e_x,h_y)$ are the eigenfields at the both lines of the FCL.

Let us now examine the four-port section of the FCL shown in Fig. 4, where microstrip ports **1, 2** and **3, 4** are located at the interfaces $z = 0$ and $z = l$, respectively. The field expansion in the ports is limited only to the two modes. There are dominant quasi-TEM $\underline{\mathbf{1}}$ and higher quasi-TE_1 $\underline{\mathbf{2}}$ modes of a single microstrip line. Note that their eigenfields can be considered as close to the ones of the isotropic modes associated with the one of the FCL line. Therefore, it is possible to express the transverse fields components at the microstrip ports of the junction as follows:

$$\vec{E}_t^n = v_1^n\vec{e} + v_2^n\vec{\tilde{e}}$$
$$\vec{H}_t^n = i_1^n\vec{h} + i_2^n\vec{\tilde{h}} \quad (9)$$

where $n = 1,\ldots,4$ refers to the port number, and superscripts 1 and 2 relate to the modes employed in the ports. Now we apply the continuity conditions for the tangential-field component of electric and magnetic fields at the interfaces $z = 0$ and $z = l$. It corresponds to the matching of the transversal field components (7) and (9) at the port interfaces when the influence of their transverse distributions on the neighboring ports can be omitted. Imposing the continuity conditions at $z = 0, l$ yields the set of equations that are dot-multiplying by conjugate values of eigenfields (e^*,h^*) and $(\tilde{e}^*,\tilde{h}^*)$, respectively, and integrated over the n-port interface. Hence, for $z = 0$, we obtain

$$\begin{bmatrix} \underline{v}_o \\ \underline{i}_o \end{bmatrix} = \begin{bmatrix} \underline{\underline{P}} & \underline{\underline{P}} \\ \underline{\underline{Q}} & -\underline{\underline{Q}} \end{bmatrix} \begin{bmatrix} \underline{A}_F \\ \underline{A}_B \end{bmatrix} = \underline{\underline{R}}_o\underline{A} \quad (10)$$

where $\underline{v}_o = (v_1^1, v_1^2, v_2^1, v_2^2)^T$, $\underline{i}_o = (i_1^1, i_1^2, i_2^1, i_2^2)^T$ and the submatrices $\underline{\underline{P}}$ and $\underline{\underline{Q}}$ are given as

$$\underline{\underline{P}} = \begin{bmatrix} 1+M_{21} & 1+M_{12} & M_{13}+M_{23} & M_{14}+M_{24} \\ 1-M_{21} & -1+M_{12} & M_{13}-M_{23} & M_{14}-M_{24} \\ M_{31}+M_{41} & M_{32}+M_{42} & 1+M_{43} & 1+M_{34} \\ M_{31}-M_{41} & M_{32}-M_{42} & 1-M_{43} & -1+M_{34} \end{bmatrix} \tag{11}$$

and

$$\underline{\underline{Q}} = \begin{bmatrix} Y_{11}+Y_{21} & Y_{12}+Y_{22} & Y_{13}+Y_{23} & Y_{14}+Y_{24} \\ Y_{11}-Y_{21} & Y_{12}-Y_{22} & Y_{13}-Y_{23} & Y_{14}-Y_{24} \\ Y_{31}+Y_{41} & Y_{32}+Y_{42} & Y_{33}+Y_{43} & Y_{34}+Y_{44} \\ Y_{31}-Y_{41} & Y_{32}-Y_{42} & Y_{33}-Y_{43} & Y_{34}-Y_{44} \end{bmatrix}. \tag{12}$$

It is conventional to assume the opposite direction of the current vectors of ports placed at the interface $z = l$. Hence, the transformations of the continuity conditions at $z = l$ yield

$$\begin{bmatrix} \underline{v}_l \\ \underline{i}_l \end{bmatrix} = \begin{bmatrix} \underline{\underline{P}} & \underline{\underline{P}} \\ -\underline{\underline{Q}} & \underline{\underline{Q}} \end{bmatrix} \begin{bmatrix} \mathrm{diag}(e^{-jk_i l}) & \underline{\underline{0}} \\ \underline{\underline{0}} & \mathrm{diag}(e^{jk_i l}) \end{bmatrix} \begin{bmatrix} \underline{A}_F \\ \underline{A}_B \end{bmatrix} = \underline{\underline{R}}_l \underline{A} \tag{13}$$

where $\underline{v}_l = (v_3^1, v_3^2, v_4^1, v_4^2)^T$ and $\underline{i}_o = (i_3^1, i_3^2, i_4^1, i_4^2)^T$.

Now we wish to eliminate the vector of unknown coefficients $\underline{A}$. From (10), it is possible to relate the $\underline{A}$ coefficients to the voltages and currents at the ports of the plane $z = 0$, assuming that the $\underline{\underline{R}}_o$ has an inverse

$$\underline{A} = \underline{\underline{R}}_o^{-1} \begin{bmatrix} \underline{v}_o \\ \underline{i}_o \end{bmatrix}. \tag{14}$$

Applying (14) in (13), the voltages and currents at the ports of the plane $z = l$ are then given by

$$\begin{bmatrix} \underline{v}_l \\ \underline{i}_l \end{bmatrix} = \underline{\underline{A}} \begin{bmatrix} \underline{v}_o \\ \underline{i}_o \end{bmatrix} \tag{15}$$

where $\underline{\underline{A}} = \underline{\underline{R}}_l \underline{\underline{R}}_o^{-1} = \begin{bmatrix} \underline{\underline{A}}_{vv} & \underline{\underline{A}}_{vi} \\ \underline{\underline{A}}_{iv} & \underline{\underline{A}}_{ii} \end{bmatrix}$ is a two modal transfer matrix of the FCL section under test. The $\underline{\underline{A}}$ matrix can be now converted into the scattering matrix $\underline{\underline{S}}$, which gives the essential power relations of the device in terms of wave amplitudes. First, we relate the voltages and currents to the wave amplitudes as

$$\begin{aligned} v_i^n &= \sqrt{Z_i}\left(a_i^n + b_i^n\right) \\ i_i^n &= \frac{1}{\sqrt{Z_i}}\left(a_i^n - b_i^n\right) \end{aligned} \tag{16}$$

where a_i^n and b_i^n represent an ith input and output wave, respectively, at the nth port. Z_i is the wave impedance of a ith wave. We assume that this impedance at all ports is identical. Next, substituting (16) into (15) and after some of the mathematical rearrangement, the two-modal scattering matrix $\underline{\underline{S}}$ of the investigated four-port FCL junction takes the form

$$\begin{bmatrix} \underline{b}_1 \\ \underline{b}_2 \end{bmatrix} = \begin{bmatrix} \underline{\underline{S}}_{11} & \underline{\underline{S}}_{12} \\ \underline{\underline{S}}_{21} & \underline{\underline{S}}_{22} \end{bmatrix} \begin{bmatrix} \underline{a}_1 \\ \underline{a}_2 \end{bmatrix} \tag{17}$$

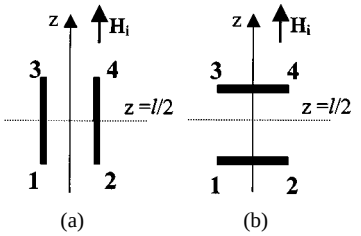

Fig. 5. Schematic representation of an FCL junction magnetized: (a) axially and (b) transversely.

where $\underline{a}_i$ and $\underline{b}$ for ith wave ($i = 1, 2$) are the four-element column vectors of the wave amplitudes at the ports, and $\underline{\underline{S}}_{ij}$ for $i, j = 1, 2$ is a complex 4×4 submatrices of the scattering matrix of interest. Furthermore, we have assumed that evanescent modes are sufficiently attenuated near the transition plane of the ports. The propagating dominant modes are then still referred to the transition planes and, for dominant mode propagation in the ports, the scattering matrix of the junction can be taken as submatrix $\underline{\underline{S}}_{1,1}$ of (17), which is read as

$$\underline{b}_1 = \underline{\underline{S}}^{\mathrm{FCL}} \underline{a}_1 \tag{18}$$

where

$$\underline{\underline{S}}^{\mathrm{FCL}} = \begin{bmatrix} S_{11} & S_{12} & S_{13} & S_{14} \\ S_{21} & S_{22} & S_{23} & S_{24} \\ S_{31} & S_{32} & S_{33} & S_{34} \\ S_{41} & S_{42} & S_{43} & S_{44} \end{bmatrix} \tag{19}$$

and the subscripts denote the junction ports.

IV. Properties of FCL Junctions

Now let us consider the influence of the symmetry plane $z = l/2$ on the scattering properties of the FCL junctions shown in Fig. 5. This plane, as perpendicular to the magnetization, can be taken as the field symmetry wall. It is a magnetic and electric wall when the ports **1, 3** or **2, 4** are reinforced by even- and odd-mode excitation, respectively. It means that the reciprocal transmission can be observed between these ports, while the transmission between the remaining ports of the junction can be nonreciprocal. From the symmetry, the following relationships can be established for the scattering matrix elements:

$$\begin{aligned} S_{11} &= S_{33} \quad S_{22} = S_{44} \\ S_{21} &= S_{43} \quad S_{12} = S_{34} \\ S_{31} &= S_{13} \quad S_{42} = S_{24} \\ S_{41} &= S_{23} \quad S_{14} = S_{32}. \end{aligned} \tag{20}$$

Applying (20) to (19) yields an $\underline{\underline{S}}^{\mathrm{FCL}}$ matrix as follows:

$$\underline{\underline{S}}^{\mathrm{FCL}} = \begin{bmatrix} S_{11} & S_{12} & S_{31} & S_{32} \\ S_{21} & S_{22} & S_{41} & S_{42} \\ S_{31} & S_{32} & S_{11} & S_{12} \\ S_{41} & S_{42} & S_{21} & S_{22} \end{bmatrix}. \tag{21}$$

Assume now that the junction [see Fig. 5(a)] is completely matched and the ports **1** and **2** and ports **3** and **4** are mutually isolated. It means that diagonal elements S_{11} and S_{22}, as well

as nondiagonal elements S_{12} and S_{21} in (21) are equal zero. The unitary property of $\underline{\underline{S}}$ then yields the equations

$$|S_{31}|^2 + |S_{41}|^2 = 1 \tag{22a}$$
$$|S_{32}|^2 + |S_{42}|^2 = 1 \tag{22b}$$
$$S_{31}S_{32}^* + S_{41}S_{42}^* = 0. \tag{22c}$$

One way for (22a)–(22c) to be satisfied is when $|S_{31}| = |S_{42}|$, which results from equal power coupling between the lines of the junction. Equations (22a) and (22b) are now employed to give $|S_{41}| = |S_{32}|$. Equation (22c) is then satisfied when the phase difference $(\phi_{31} - \phi_{32}) - (\phi_{41} - \phi_{42}) = \pm 180°$. Hence, we obtain $|(\phi_{31} - \phi_{41}) - (\phi_{32} - \phi_{42})| = 180°$ independent of FCL parameters. If we choose the reference planes of the four ports so that $\phi_{31} = \phi_{42} = \phi, \phi_{32} = \phi + \varphi_{32}$ and $\phi_{41} = \phi + \varphi_{41}$, then from (22c), it can be shown that $|\varphi_{32} + \varphi_{41}| = 180°$. Hence, the nonreciprocal phase shift occurs in FCL when $\varphi_{32} \neq \varphi_{41}$. There is the optimal nonreciprocal effect when $\varphi_{32} = 0°$ or 180° and $\varphi_{41} = 180°$ or 0°, respectively. It implies a gyrator effect between the FCL ports **1** and **4**, as well as **2** and **3**. Obviously, it makes it possible to use the FCL sections in the design of nonreciprocal devices. Consider now the other way that allows one to satisfy the equations resulting from unitary conditions of (21). We introduce the matching conditions and assume that the ports **1, 3** and **2, 4** connected by the lines are now isolated. The elements S_{11}, S_{22} and S_{31}, S_{24} are then equal to zero and the unitarity of (21) yields the following equations:

$$\begin{aligned} |S_{12}|^2 + |S_{32}|^2 &= 1 \\ |S_{21}|^2 + |S_{41}|^2 &= 1 \\ S_{21}S_{41}^* + S_{41}S_{21}^* &= 0 \\ S_{12}S_{32}^* + S_{32}S_{12}^* &= 0. \end{aligned} \tag{23}$$

Here, we have two solutions of (23), i.e., $|S_{21}| = |S_{32}| = 1$ or 0 and $|S_{12}| = |S_{41}| = 0$ or 1. It indicates the operation of the structure as a four-port circulator. However, the assumption that the ports connected here by the lines are uncoupled cannot be accepted because the signal transmission between these ports will be observed. Hence, the circulation effect should not be expected in the considered FCL configuration shown in Fig. 5(a). Now we consider another model of the FCL [see Fig. 5(b)] in which the ports **1, 2** and **3, 4** are coupled by the lines, whereas ports **1, 3** and **2, 4** are disconnected. It means that the mentioned isolation condition can be satisfied and the circulation effect can be met in this configuration. Thus, this configuration relates to the experimental FCL structure investigated in [10], where the circulation effect was confirmed and qualitatively explained. However, the different field phenomena determine the operation principle of the considered FCL structures. The Faraday phenomenon is possible in the axially magnetized FCL, while the field displacement effect occurs in the transversely magnetized structure. Therefore, the other CM model is needed to explain the operation principle of the transversely magnetized FCL. Indeed, the CM model of the FCL presented here can be used only to design the axially magnetized FCL junction shown in Fig. 5(a).

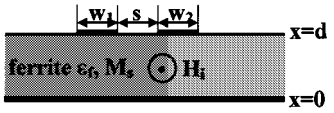

Fig. 6. Cross section of the ferrite section of the microstrip FCL junction presented in Fig. 4. Structure parameters in the text follow from [7].

V. Numerical Results

Having defined the scattering model of the microstrip FCL structure, we now investigate the behavior of the microstrip ferrite four-port junction that was designed and measured by Davis *et al.* in [7]. For the design of the junction, they applied new normal-mode conditions, which they recently developed in [6] for the model of the FCL. These conditions allowed one to find not only the optimal length of the ferrite section, but to also estimate the matching properties of the FCL junction. For realization of the junction, they have applied the section of ferrite coupled microstrips whose cross section is given in Fig. 6. It is made on a saturated $(H_i = 0)$ ferrite substrate with saturation magnetization $M_s = 141$ kA/m, dielectric permittivity $\varepsilon_f = 15$, and thickness $d = 0.635$ mm. The widths of the microstrips are $w = 0.6$ mm and they are separated by the slot $s = 0.5$ mm.

The microstrip ports of the junction are designed on the dielectric substrate with $\varepsilon_d = 9.8$ and have the same dimensions as the ferrite microstrip lines. The measured responses of the FCL junction of 48-mm length are presented in [7, Figs. 4 and 5]. These results indicate that the considered FCL operates optimally near the 6.6-GHz frequency where most of the signal energy is transmitted to one of the output ports for even (or odd)-mode excitation. It only confirms the power exchange ability of the two-coupled lines resulting from Faraday's rotation effect of the ferrite section. Note that a similar, but reciprocal effect can appear at the sections of the coupled lines containing, for example, anisotropic medium, where the change of the polarization state of the wave is possible. Therefore, the nonreciprocal behavior of the FCL can be identified only in the case when the phase shift additionally occurs for the reverse direction of magnetization on the FCL. In such a case, the rotation direction is reversed and the signal energy should be transmitted to the second output port of the FCL. However, this effect has not been measured in [7] where the properties of the structure are presented only for one direction of the magnetization. The normal-mode approach [6] was developed [7] to model the behavior of the measured FCL junction. The results are presented in [7], showing good agreement between the experimental and theoretical values of the operation frequency (6.6 GHz) estimated for minimum reflection. It indicates, in principle, that theory [6] can be applied to the design and optimization of the microstrip FCL section. However, values of the scattering characteristics theoretically predicted in [7] did not agree well with the measured ones. For comparison, their measured values of insertion loss and isolation at 6.6 GHz are approximately 1.5 dB and better then 30 dB, whereas the calculated ones are 0.4 and 11 dB, respectively. Such disagreement could be expected since theory [6] concerned the FCL, whose second interface was perfectly matched. In our opinion, even small reflection from the second FCL interface can provide such differences. Therefore,

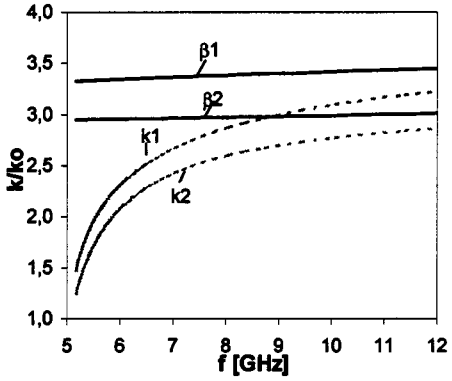

Fig. 7. Dispersion characteristics of the dominant ferrite and isotropic modes of the microstrip FCL shown in Fig. 6 (spectral-domain approach). Propagation coefficients of isotropic modes: β_1, β_2 and ferrite modes: k_1, k_2.

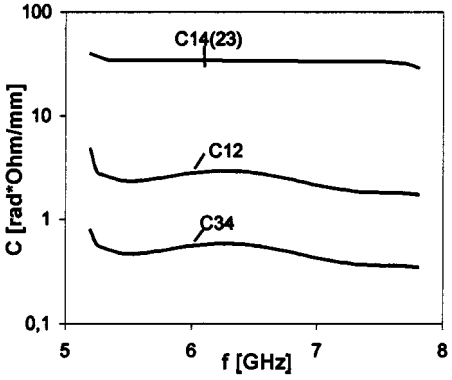

Fig. 8. Computed coupling coefficients $C_{12}, C_{13} = C_{24}, C_{34}$ for the microstrip FCL shown in Fig. 6.

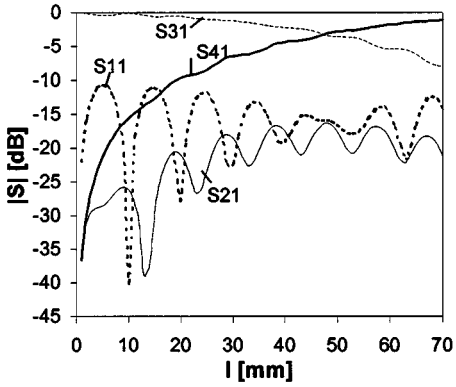

Fig. 9. Computed scattering parameters of (Davis *et al.*) microstrip FCL junction (see Figs. 4 and 6) at the frequency $f = 6.6$ GHz for different length of the ferrite section (signal enters port **1**).

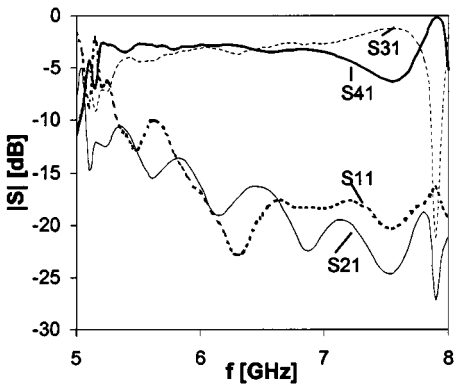

Fig. 10. Frequency-dependent scattering characteristics of the (Davis *et al.*) microstrip FCL junction (see Figs. 4 and 6). The length of the ferrite section is equal to 48 mm. The junction is excited from port **1** of the FCL.

the CM model presented here will be now applied to reexamine the properties of the FCL junction investigated in [7]. According to CM requirements, the wave parameters of the isotropic modes and the coupling coefficients are needed to model the junction. Using the spectral-domain theory solution of the ferrite microstrip-line structure (see Fig. 6), we have computed the propagation coefficients of ferrite and isotropic modes. The complete dispersion characteristics of dominant ferrite and isotropic modes are presented in Fig. 7. Having defined the values of propagation coefficients of both ferrite and isotropic modes, we have solved the system of characteristic equations of (4a) to determine the coupling coefficients. Their frequency response is shown in Fig. 8. We can see that they decrease in the range beyond the cutoff frequencies of the dominant ferrite modes. It attests that the investigated FCL operates above, but near, the cutoff frequencies. We now reexamine the properties of the FCL under test, assuming that its ports are terminated with wave impedance of the external isotropic microstrips. First, we calculate the variation of the scattering parameters of the FCL versus the length of the ferrite section at the fixed 6.6-GHz frequency. The results are shown in Fig. 9.

The important effect we observe is the exchange of the signal energy between both lines of the structure. The recommended length of the FCL is defined for a symmetrical split of the energy, which appears here for a length of 47 mm. It is worth noting that this value agrees well with the 48-mm length predicted in [7]. However, we shall investigate (Davis *et al.*) the FCL junction of 48-mm length.

Fig. 10 shows the frequency dependent scattering characteristics calculated for excitation of the junction in port **1**. Note that an almost symmetrical split of the energy occurs in the frequency band from 6.2 to 6.7 GHz. If the phase difference between the output signals S_{31} and S_{41} is equal to 0° or 180°, then an even or odd mode can be seen at the output ports. It was found that the excitation in port 1 results in the even mode emerging at ports **3** and **4**. The similar transmission is observed when the structure is excited in port **3**, while the wave incident in port **2** or **4** produces in the output ports the field distribution corresponding to the odd mode. The converse effect occurs if the biasing magnetic field is reversed. Additional computation was carried out for even and odd excitation of the junction. The results are presented in Fig. 11, showing agreement between our theory and the experimental values of [7]. Divergences occur mainly between the measured and calculated operation frequency of 6.6 and 6.45 GHz, respectively. The measured isolation is closer to our theoretical value than to the ones presented in [7]. For example, our theory, as well as experiment, shows that the isolation at the operation frequency is higher than 25 dB. It was also found that, for reverse magnetization, the

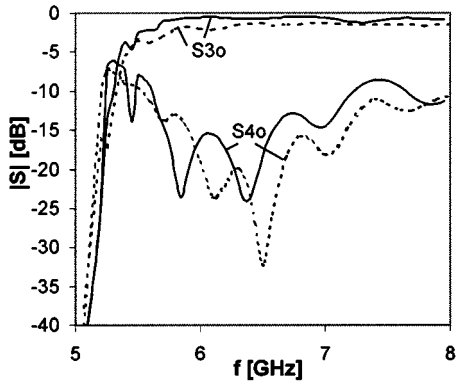

(a)

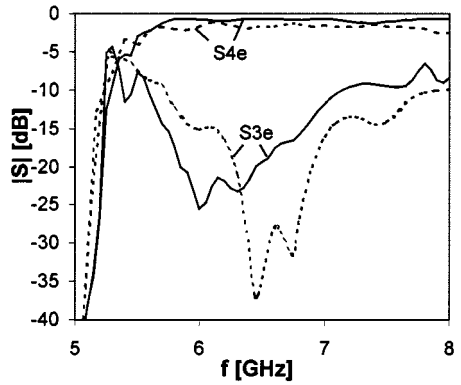

(b)

Fig. 11. Computed insertion loss and isolation of the (Davis *et al.*) microstrip FCL junction (see Figs. 4 and 6) for: (a) odd- and (b) even-mode input at the ports **1** and **2**. Comparison with experimental results from [7] (dashed lines: experiment [7], solid line: CM theory).

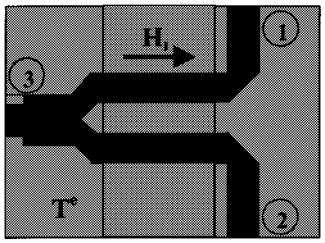

Fig. 12. Schematic representation of the circuit of a three-port distributed microstrip FCL circulator simulated as a cascade of the investigated FCL and microstrip T^e junction. Ports impedance $Z_o \sim 50\ \Omega$. Details given in the text.

excitations of the junction by the even and odd mode give an output at the opposite ports of those presented in Fig. 11. This result clearly shows the FCL nonreciprocal behavior required for the three-port circulator. The three-port circulator consists of an FCL junction in cascade with a hybrid T, as shown in Fig. 12. Thus, the T-junction ensures even-mode excitation of the FCL, which is in need of circulator operation.

We simulated a T-structure realized on the same dielectric substrate as the input sections of the FCL junction. Its coupled dielectric microstrip lines feeding FCL have the same dimensions as ferrite lines, and they are 5 mm in length. The quarter-wave transformer (see Fig. 12) is used to match the characteristic impedance 29.4 Ω of a T-junction input line and impedance $Z_o = 50\ \Omega$ of port **3**. In Fig. 13, the scattering characteristics of the hybrid T-junction are shown as the function

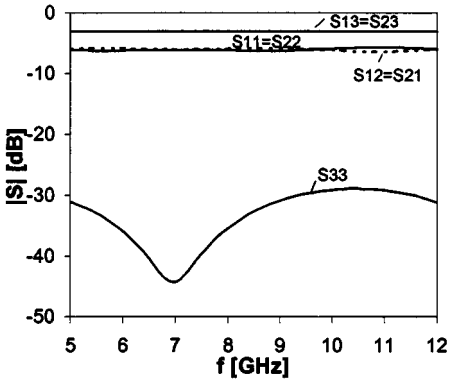

Fig. 13. Scattering characteristics of the microstrip T^e junction used in the structure of the FCL circulator shown in Fig. 12.

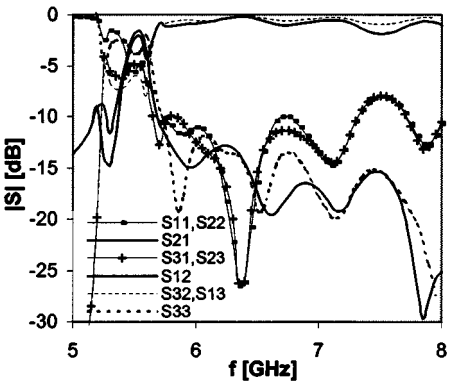

Fig. 14. Performance of the distributed FCL circulator presented in Fig. 12.

of frequency. The best operation is seen in the 6–7-GHz band, where the even-mode output from its ports **1** and **2** is evident. The overall scattering matrix of the circulator is calculated by combining directly the appropriate scattering matrices of the cascaded T-junction and four-port FCL. S-parameter characteristics are shown in Fig. 14, where the three-port circulator behavior is clearly presented. In particular, the computed characteristics demonstrate asymmetrical operation of the device. For FCL circulators, this effect was previously predicted in [4]. It can be seen that maximum isolations S_{31} and S_{23}, together with return losses S_{11} and S_{22} are better than 25 dB at the operation frequency of $f = 6.4$ GHz. However, values of these parameters decrease to 15 and 12 dB at the 6.6- and 5.7-GHz frequencies, respectively. At these frequencies, the isolation S_{12} and return loss S_{33} of 19 dB are obtained. One should note that the isolations and return losses of the circulator varying between 10–20 dB at the 5.7–7.3-GHz frequency band with maximum 1.5-dB insertion losses over this range. These initial results were obtained for a nonoptimized structure. Although the result is not very encouraging to promote the microstrip FCL circulator, it proves, however, the validity of the conception of this device design and shows that further work is needed to allow one to design the optimal structure.

VI. Conclusion

The CM method has been successfully applied to solve the eigenvalues problem of axially magnetized ferrite-coupled microstrip lines. On the basis of gyromagnetic coupling between

the dominant propagating and higher order evanescent isotropic modes, the eigenmode solution of the FCL was found to bear through their decomposition of the eigenfields at each line of the guide. The results of the analysis were used to derive a scattering matrix for the four-port FCL junction. This problem was solved by matching the fields of isotropic and ferrite waves at each port of the investigated junction. Considering the symmetry property of the structure with respect to the magnetization direction, the general nonreciprocal performance of the axially and transversely magnetized FCL junction has been discussed. Verification of the modeling was demonstrated by comparing numerical results with an experiment presented in [7]. The good agreement with experimental results indicates that the presented model can be used in microstrip FCL junction design. It makes it possible to investigate the novel nonreciprocal devices comprising the section of the FCL. As an example, the three-port circulator constructed as the cascade of the microstrip T-junction and FCL section has been described with promising scattering performance.

REFERENCES

[1] L. E. Davis and D. B. Sillars, "Millimetric nonreciprocal coupled-slot fin-line components," *IEEE Trans. Microwave Theory Tech.*, vol. MTT-34, pp. 804–808, July 1986.

[2] J. Mazur and M. Mrozowski, "On the mode coupling in longitudinally magnetized waveguide structures," *IEEE Trans. Microwave Theory Tech.*, vol. 37, pp. 159–164, Jan. 1989.

[3] ——, "Nonreciprocal operation of structures comprising a section of coupled ferrite lines with longitudinal magnetization direction," *IEEE Trans. Microwave Theory Tech.*, vol. 37, pp. 1012–1019, July 1989.

[4] C. S. Teoh and L. E. Davis, "Normal-mode analysis of ferrite-coupled lines using microstrips and slotlines," *IEEE Trans. Microwave Theory Tech.*, vol. 43, pp. 2991–2998, Dec. 1995.

[5] ——, "Normal-mode analysis of ferrite-coupled lines using microstrips and slotlines," in *IEEE MTT-S Int. Microwave Symp. Dig.*, Orlando, FL, May 15–19, 1995, pp. 99–102.

[6] K. Xie and E. Davis, "Nonreciprocity and the optimum operation of ferrite coupled lines," *IEEE Trans. Microwave Theory Tech.*, vol. 48, pp. 562–573, Apr. 2000.

[7] E. Davis *et al.*, "Design and measurement of ferrite coupled line circulators," in *Proc. IEEE MTT-S Int. Microwave Symp. Dig.*, vol. 3, June 1999, pp. 1153–1156.

[8] D. Marcuse, "Coupled-mode theory for anisotropic optical guide," *Bell Syst. Tech. J.*, vol. 54, pp. 985–995, May 1973.

[9] J. Mazur, P. Kutysz, and A. Cwikla, "Coupled-mode analysis of ferrite microstrip lines," *IEEE Microwave Guided Wave Lett.*, vol. 9, pp. 300–302, Aug. 1999.

[10] I. Awai and T. Itoh, "Coupled-mode theory analysis of distributed nonreciprocal structures," *IEEE Trans. Microwave Theory Tech.*, vol. MTT-29, pp. 1077–1086, Oct. 1981.

Jerzy Mazur was born in Brno, Czech Republic, on March 23, 1946. He received the M.Sc.E.E. degree and the Ph.D. and habilitation degrees in electrical communication engineering from the Technical University of Gdańsk (TUG), Gdańsk, Poland, in 1969, 1976, and 1983, respectively.

He is currently a Full Professor at TUG. Since 1992, he has been also a consultant to the Telecommunication Research Institute, TUG. His research interests are concerned with electromagnetic field theory and integrated circuits for microwave and millimeter-wave applications.

Mateusz Mazur was born in Gdynia, Poland, in 1975. He received the M.Sc.E.E. degree from the Technical University of Gdańsk (TUG), Gdańsk, Poland, in 1999.

He is currently with the Telecommunication Research Institute, TUG. His research interests include numerical methods and development of wide-band and phased-array antennas for radar systems application.

Jerzy Michalski received the M.Sc.E.E. degree from the Technical University of Gdańsk (TUG), Gdańsk, Poland in 1998, and is currently working toward the degree at the Telecommunication Research Institute.

His research interests are wave propagation in complex materials and nonreciprocal planar microwave devices.